

Exploring and Evaluating Real-world CXL: Use Cases and System Adoption

Jie Liu*

University of California, Merced
Merced, CA, USA
jliu279@ucmerced.edu

Shuangyan Yang

University of California, Merced
Merced, CA, USA
syang127@ucmerced.edu

Xi Wang*

University of California, Merced
Merced, CA, USA
swang166@ucmerced.edu

Jie Ren

William & Mary
Williamsburg, VA, USA
jren03@wm.edu

Jianbo Wu

University of California, Merced
Merced, CA, USA
jwu323@ucmerced.edu

Bhanu Shankar

MemVerge, Inc
Milpitas, CA, USA
bhanu.shankar@memverge.com

Dong Li

University of California, Merced
Merced, CA, USA
dli35@ucmerced.edu

Abstract

Compute eXpress Link (CXL) is emerging as a promising memory interface technology. Because of the common unavailability of CXL devices, the performance of the CXL memory is largely unknown. What are the use cases for the CXL memory? What are the impacts of the CXL memory on application performance? How to use the CXL memory in combination with existing memory components? In this work, we study the performance of three genuine CXL memory-expansion cards from different vendors. We characterize the basic performance of the CXL memory, study how HPC applications and large language models can benefit from the CXL memory, and study the interplay between memory tiering and page interleaving. We also propose a novel data object-level interleaving policy to match the interleaving policy with memory access patterns. We reveal the challenges and opportunities of using the CXL memory.

1 Introduction

Compute eXpress Link (CXL) is emerging as a promising memory interface technology. Based on the standard PCIe serial interface, CXL can attach memory to the CPU and appears to a system as a CPU-less NUMA node. This introduces flexibility in memory subsystem design and fine-grained control over memory bandwidth and capacity.

Compared with the traditional memory interface technology (such as DDR), CXL provides multiple benefits. *First*, CXL provides a more scalable method than DDR to increase memory capacity and bandwidth, because CXL does not increase the number of DDR channels or cause super-linear increase of energy consumption and signaling challenges as DDR [49]. *Second*, the CXL memory provides a solution to avoid memory stranding [27], because using the CXL memory as a pool,

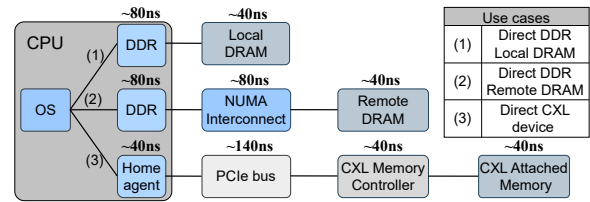


Figure 1. Breakdown of CXL memory access latency.

the stranded memory can be disaggregated from servers and provide memory capacity as demanded. *Third*, with CXL, the memory technologies are decoupled from the memory interface technologies used by the CPU [56, 60, 62], which provides unprecedented flexibility to reuse old memory and build the memory pool. *Fourth*, CXL allows the CPU to communicate with the attached memory in a cache-coherent fashion using load and store instructions. This is aligned with the traditional memory semantics, and hence provides conveniences of using existing programming models and system designs (e.g., NUMA-based tiered memory). *Fifth*, data fetched from and written to the CXL memory can be cached in the cache hierarchy in the CPU, which allow the system to explore locality for higher performance. This contrasts with RDMA where data cannot be cached in the CPU.

However, CXL memory introduces longer memory access latency. This longer latency comes from PCIe, CXL memory controller, and CXL home agent (HA) on the CPU. Figure 1 compares local NUMA, traditional remote NUMA, and CXL-based memory expansion in terms of memory latency. It has been reported that the CXL adds about 70-150 ns of extra latency over normal DRAM access [32].

Given the CXL performance, we face a series of questions: what are the use cases for the CXL memory? What are the impacts of real CXL memory on application performance?

*Co-first author

At the application level, how to use the CXL memory in combination with fast memory components (e.g., using uniform page-level interleaving vs. data object-level interleaving vs. memory binding)? This paper aims to discuss those questions, characterize the performance of the CXL memory, and explore various paths to use the CXL memory. We study three genuine CXL memory expansion cards from different vendors, and have the following insights.

The CXL memory is a unique “NUMA node”. The CXL memory appears as a CPU-less NUMA node. In the three systems we evaluate, the CXL memory appears as a two-hop-away NUMA node in terms of access latency. Depending on the memory vendors, the peak bandwidth of the CXL memory varies a lot, ranging from 9.8% to 80.3% of the peak bandwidth of local DRAM. In addition, as we scale the number of threads to access the CXL memory, its memory bandwidth is easily saturated because of PCIe (the saturation point is reached when the number of threads is only 4), while local DRAM (or LDRAM for short) and remote DRAM-based NUMA node (or RDRAM for short) have much better scalability. This scaling difference between the CXL memory and DRAM highlights the importance of appropriately distributing memory accesses between them for high performance. Also, when the system is under heavy load, we notice that LDRAM and RDRAM can show the similar latency as the CXL memory because of the contention on the memory controller (MC) or data path, which shows the potential of using CXL as LDRAM or RDRAM for latency-sensitive applications when the system is under heavy load.

HPC applications can benefit a lot from the CXL memory for high performance while saving fast memory. Our work goes beyond the existing work [49] that focuses on applications exhibiting *ms*-scale latency (e.g., social network microservices) to study the potential of the CXL memory. We study a spectrum of HPC workloads, covering the most common and representative “HPC dwarfs” [5]. We reveal that some HPC applications (such as CG and BT [30]) can tolerate low bandwidth and high latency of the CXL memory under certain scales (the performance loss is less than 3.2%, compared with LDRAM), because of their compute-intensive nature.

In addition, the page interleaving policy, embraced by the industry (e.g., Micron and AMD [34], Astera Labs [22], and Samsung [35]) as an application-transparent technique to integrate CXL with the existing memory components, provides opportunities to save LDRAM for HPC applications. When interleaving CXL and RDRAM, we see minor performance difference from interleaving CXL and LDRAM for some applications. This is because the CXL memory dominates the memory performance, and the performance of other memory components has minor impact on the overall performance.

To maximize the interleaving performance, we propose a data object-level interleaving policy. This policy decides whether memory pages allocated to a data object should be

interleaved between CXL and DRAM or allocated to LDRAM first (“LDRAM preferred”). This policy maximizes memory bandwidth (or minimize latency) for data objects whose accesses favor high bandwidth (or low latency). This policy reduces the usage of fast memory (LDRAM) by 48% on average and outperforms the uniform interleaving policy (the Linux policy) by 65% on average.

Using the CXL memory for large language models (LLM) faces challenges. We study the cases that use the CPU memory as an extension to the GPU memory to enable LLM training (using ZeRO-Offload [40]) and inference (using FlexGen [46]) such that we can use less GPUs for LLM without the constraint of GPU memory capacity. This method has to frequently copy tensors between the GPU and the CPU, and offloads certain computations from the CPU to the GPU to maximize GPU memory saving or reduce I/O offload. This method (named *tensor offloading* in the rest of the paper) has been commonly studied and deployed in industry.

We find that using tensor offloading based upon the CXL memory brings limited performance improvement. This is because the tensor copy between the CXL memory and GPU memory goes through a longer data path than memory accesses directly from CPU. Using CXL 1.1 on our platform, this data path is bottlenecked by the PCIe interconnect between CPU and GPU. As a result, adding CXL cannot show the bandwidth benefits for tensor offloading. In contrast, the computation offloaded to the CPU (i.e., the optimizer for LLM training and the attention computation for LLM inference), which tends to be bandwidth sensitive, can benefit from the extra bandwidth of CXL. In addition, the CXL memory increases memory capacity and allows us to use larger batch sizes for LLM inference, leading to throughput gains.

Memory tiering solutions need to be improved. Treating the CXL memory as a memory tier, existing work [10, 24, 32, 37, 41, 53] migrates pages between the CXL memory and fast memories based on page access frequency or recency (i.e., hotness). Those solutions are seldom studied with the real CXL memory, and how they interplay with the existing system (e.g., page interleaving) is largely unknown.

We find that the dynamic page migration in the memory tiering solutions are not integrated well with the static page interleaving, because of invalidness of NUMA hint faults. Depending on the temporal and spatial distribution of hot pages, the dynamic page migration can degrade application performance compared to no migration. We also observe that the old-fashioned NUMA first touch and Tiering-0.8 [53] (the most recent Linux Patch for AutoNUMA to support memory tiering) is very effective, outperforming a set of page migration and interleaving solutions.

Table 1. Three systems with CXL devices.

Sys	Component	Description
A	OS (kernel)	Ubuntu 22.04 LTS (Linux kernel v6.2.15)
	CPUs	2× AMD EPYC 9354 CPUs @3.8 GHz, 32 cores and 512 MB LLC per CPU
	PCIe	PCIe 5.0, speed 32GT/s, 16 lanes
	Memory	Socket 0: 12× DDR5-4800 channels, memory 768GB Socket 1: 12× DDR5-4800 channels, memory 768GB
	CXL A	Single channel DDR5-4800, memory 128 GB, max bandwidth 38.4 GB/s per channel
B	OS (kernel)	Fedora Linux 36 (Linux kernel v6.6.0-rc5)
	CPUs	2× Intel(R) Xeon(R) Platinum 8470 CPU @2.0GHz, 52 cores and 210 MB LLC per CPU (Sapphire Rapids)
	PCIe	PCIe 5.0, speed 32GT/s, 16 lanes
	Memory	Socket 0: 8× DDR5-4800 channels, memory 1TB Socket 1: 8× DDR5-4800 channels, memory 1TB
	CXL B	Single channel DDR5, memory 64 GB, max bandwidth 64.0 GB/s per channel
C	OS (kernel)	Ubuntu 22.04 (Linux kernel v6.2.15)
	CPUs	2× Intel(R) Xeon(R) Gold 6438Y+ @2.0GHz, 32 cores and 60 MB LLC per CPU
	PCIe	PCIe 5.0, speed 32GT/s, 16 lanes
	Memory	Socket 0: 8× DDR5-4800 channels, memory 512GB Socket 1: 8× DDR5-4800 channels, memory 512GB
	CXL C	Dual channel DDR5-6200, memory 128 GB, max bandwidth 48.4 GB/s per channel

2 Background

2.1 Compute Express Link

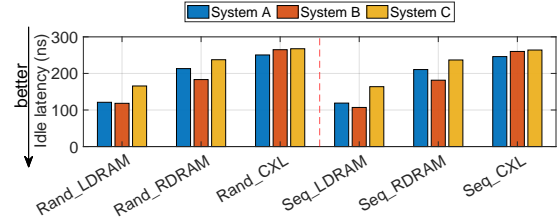
The CXL specification defines three protocols: CXL .io for initial discovery and configuration of CXL devices, CXL .cache for CXL-devices to access the host memory using PCIe protocol features, and CXL .mem for the host access to CXL device memory. The Home Agent (HA) on the CPU and CXL controller on the device manage the interaction between the host and CXL device. The HA administers the CXL .mem protocol and seamlessly presents the CXL memory to the host as memory on a remote NUMA node.

There are three types of CXL devices. The type-3 device is related to our evaluation. Such a device supports CXL .io and CXL .mem, and is used for memory bandwidth or capacity expansion, and storage class memory in memory tiering.

CXL .mem provides three coherence models for CXL exposed host-managed device memory (HDM): HDM-H (host-only coherent and used for type-3), HDM-D (device coherent relying on CXL .cache to manage coherence with the host and used for type-2), and HDM-DB (device coherent using back-invalidation and used for type-2 or type-3).

The CXL specification has been going through three major versions: 1.1, 2.0, and 3.0. 1.1 focuses on directly-attached CXL devices, 2.0 incorporates switch-based pooling, and 3.0 supports switch-less pooling and higher bandwidth.

Most of the real CXL devices nowadays are *HDM-H using CXL 1.1*. The three devices for our evaluation are among them.

**Figure 2.** Load latency with random and sequential memory accesses to a cache block.

2.2 CXL Systems for Evaluation

CXL requires compatible hardware in both the CPUs and peripheral devices. Notably, the 4th-generation Intel Xeon Scalable Processors (such as Sapphire Rapids) and the 4th-generation AMD EPYC Processors (such as Genoa) are among the first mainstream server CPUs to support the CXL 1.1. Several CXL memory devices have been developed as commercial products by leading hardware manufacturers such as SK hynix, Astera Labs, Montage, Samsung, and Micron. We use three CXL devices from three vendors. Table 1 summarizes the three systems equipped with the devices.

The system A listed in Table 1 has two sockets (0 and 1), and a CXL device is attached to the socket 1 by a CXL link over PCIe 5.0. This system has two AMD EPYC 9354 CPUs. Accessing the CXL memory from CPU 0 has to go through the HyperTransport interconnect, which leads to longer latency than accessing from CPU 1. Different from the traditional NUMA node, the CXL memory device lacks CPU cores and caches, and does not have an expensive interconnect between the CXL IP and the device’s memory controller. Hence, the CXL memory is represented as a CPU-less NUMA node in the system A. From the view of a CPU, there are three NUMA nodes: local DDR (or LDRAM), remote DDR on the other socket (RDRAM), and CXL memory. The system B has the same organization as the system A. The system C has a slightly different organization: the CXL device is attached to the socket 0 (instead of socket 1).

3 Basic Performance Characteristics

Evaluation methodology. We evaluate memory latency and bandwidth using Intel Memory Latency Checker (MLC) [15]. MLC disables hardware prefetcher for Intel processors (the systems B and C), but cannot do so for AMD processors (the system A). For latency tests, MLC uses typical pointer chasing. For each latency test, we repeat the test by 5,000 times, and report the average value after excluding outliers (caused by operating system services and random TLB misses). For bandwidth tests, we use MLC to perform sequential and random memory accesses. The sequential accesses in combination with thread-level parallelism introduces parallel memory accesses, revealing peak memory bandwidth. For each bandwidth test, we repeat the test by 2,000 times, and report the average value.

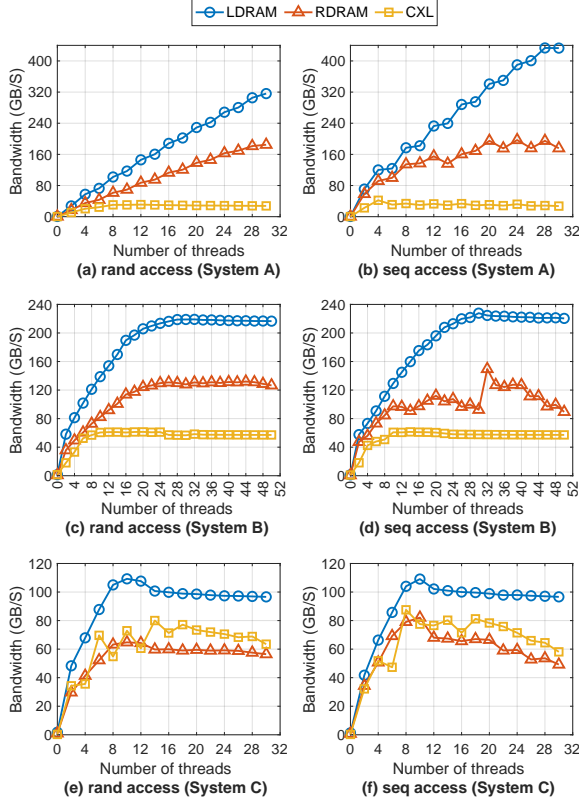


Figure 3. Bandwidth scaling for data loading.

Latency results. See Figure 2. We have two observations.

Basic observation 1. Compared with LDRAM, CXL is much slower than one-hop-away NUMA node (RDRAM). For example, for sequential accesses, compared to LDRAM, CXL increases the latency by 2.8 \times , 2.4 \times , and 2.2 \times on the three systems respectively, while one-hop-away NUMA increases the latency by 1.8 \times , 1.7 \times , and 1.5 \times . In fact, assuming that adding a hop of NUMA distance introduces a constant latency in a system, *the CXL memory is comparable to a two-hop-away NUMA node, in terms of access latency.*

Basic observation 2. Figure 2 shows that the CXL memory from different vendors show quite different latency. For example, for sequential accesses, the CXL memory in the system A adds latency by 153 ns, while the CXL memory in the system B adds latency by 211 ns, compared to LDRAM. Since the two systems use the same PCIe and DRAM technologies, such a latency difference mainly comes from the difference in the CXL controller and HA on the CPU.

Bandwidth results. Figure 3 shows the bandwidth scaling as we change the number of threads. We have three observations.

Basic observation 3. The CXL memory bandwidth is saturated as the number of threads is over 8, while the saturation points for LDRAM and RDRAM are much higher than that in CXL (e.g., 28 and 20 on the system B), indicating that the CXL memory bandwidth is limited by PCIe.

Basic observation 4. The peak CXL memory bandwidth is much lower than that of LDRAM (the CXL memory bandwidth is 9.8%, 28.1%, and 80.3% of LDRAM bandwidth on the systems A, B, and C respectively). The peak CXL memory bandwidth is also lower than that of RDRAM (the CXL memory bandwidth is 17.1% and 46.4% of the RDRAM bandwidth on the systems A and B respectively), but can be pretty close to the RDRAM bandwidth (see the system C).

Basic observation 5. Difference in bandwidth scaling between LDRAM, RDRAM, and CXL highlights the importance of distributing memory accesses between them. For example, in the system B, to maximize the bandwidth usage, we would assign 6, 23, and 23 threads to access CXL, LDRAM, and RDRAM respectively. *This leads to a peak bandwidth of 420 GB/s, larger than any other thread assignment.*

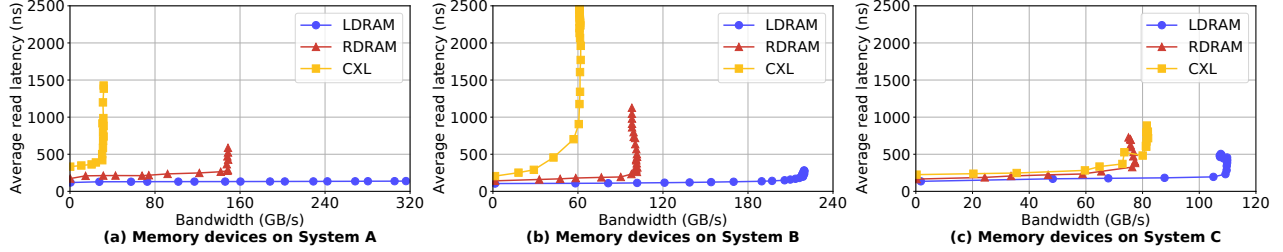
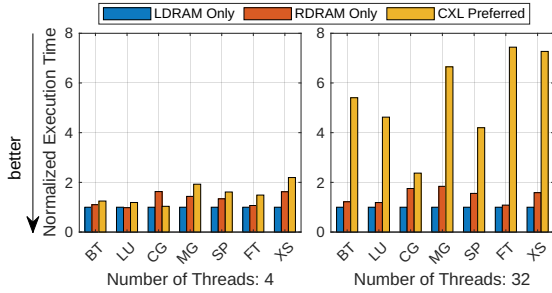
Performance under load. We study memory latency and bandwidth under varying load. Figure 4 presents the results of how latency and bandwidth vary by gradually increasing the load on memory. For this test, we employ Intel MLC, utilizing 32 threads. In our methodology, each thread performs memory accesses to cache lines and delays for a time interval between two accesses. We vary the time interval from 0 to 80 μ s. This setup ensures that each worker thread is engaged in repeated, sequential memory accesses, allowing for a detailed analysis of how varying load conditions impact memory performance. When the time interval is 0 (corresponding to the right side of each subfigure in Figure 4), the bandwidth is close to the maximum bandwidth and the latency skyrockets as the queuing effects in hardware dominate. When the time interval is high enough (80 μ s, corresponding to the left side of each subfigure in Figure 4), the latency is close to the raw, unloaded latency.

Basic observation 6. The latency of accessing LDRAM and RDRAM can be similar to the CXL memory when reaching their peak memory bandwidth. For example, in Figure 4.(c), once the bandwidth consumption of LDRAM and RDRAM approaches the peak (110GB/s for LDRAM and 84GB/s for RDRAM), their latencies are as high as 543 ns and 600 ns respectively, which are pretty close to the CXL memory latency (400 ns - 550 ns) when approaching the peak bandwidth of the CXL memory under heavy load. *This demonstrates the potential of using CXL as LDRAM and RDRAM when the system is under heavy load.*

Takeaway: CXL memory performs as a NUMA node with latency similar to RDRAM but much lower (or comparable) bandwidth. But different from the traditional NUMA node, the CXL memory is unique in terms of performance scalability and performance under heavy load.

4 HPC Workloads

We analyze HPC workload performance to demonstrate the use case of CXL memory, focusing on seven workloads from


Figure 4. Memory latency and bandwidth under varying load.

Figure 5. The overall performance for all benchmarks using various memory components. “XS” stands for “XSbench”.

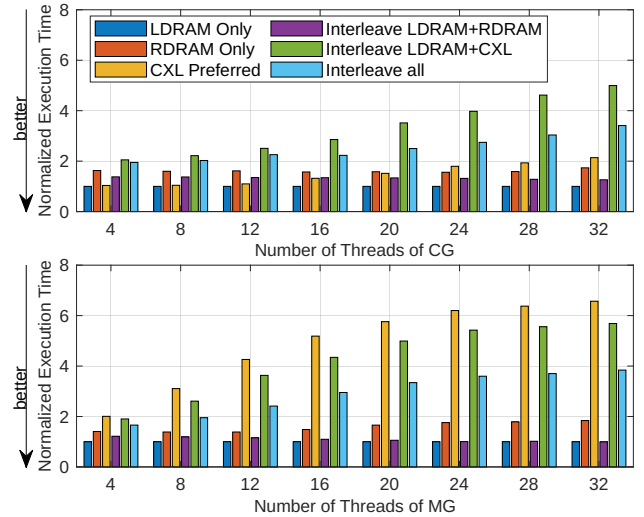
NPB benchmark suite [30] and XSbench benchmark [51]. These workloads, which require processing a large working memory set using multiple threads, are summarized in Table 2. They collectively cover the most common and representative HPC applications [5]. In our study, we use various memory allocation policies, including preferred and interleaving. The preferred policy for a specific memory node indicates that the memory is allocated in that memory node first; when that memory node runs out of space, the page allocation goes to another memory node closet to the CPU according to the NUMA distance. The interleaving policy indicates that pages are allocated among memory nodes in a round robin fashion. We present evaluation results on the system A, because its performance is between the performance of the systems B and C, hence can be representative.

4.1 Evaluation Results

HPC observation 1. Using CXL preferred, some HPC applications show minor performance loss, compared to using LDRAM and RDRAM.

Figure 5 shows the performance. We observe that BT and LU, when the number of threads is small (4), the performance difference between LDRAM and CXL preferred is very small (less than 3.2%). These benchmarks are highly compute intensive and not sensitive to long memory latency and bandwidth with a small number of threads. These results show great potential of using CXL memory to save LDRAM. For other benchmarks, the performance difference can be up to 1.9× when the number of threads is 4.

We also notice that when the number of threads is large (32), the performance difference between LDRAM and CXL


Figure 6. The scalability study for CG and MG. The performance is normalized by that of using LDRAM only.

preferred is at least 1.9×, and the performance difference between RDRAM and CXL preferred is at least 1.1×. When the number of threads is large, the memory-level parallelism imposes high pressure on memory components, exacerbating inferior performance of the CXL memory.

HPC observation 2. Bandwidth-sensitive and latency-sensitive applications respond differently to the bandwidth increase offered by CXL.

Figure 6 shows the results for MG (bandwidth-sensitive) and CG (latency-sensitive). For MG, we see that when the number of threads increases from 4 to 32, the performance of “interleave all” (i.e., interleaving between LDRAM, RDRAM and CXL, which achieves the highest bandwidth) is consistently better than that of CXL preferred by 10%-85%. Meanwhile for CG, the performance of “interleave all” performs worse than that of CXL preferred by up to 1.6×, because using CXL preferred, consecutive memory accesses tend to fall into the same memory node, which is favored by CG for high performance (see more discussions for HPC observation 4).

HPC observation 3. When the interleaving policy involves the CXL memory, we can save local fast memory by using remote fast memory.

Figure 7 shows the results with various interleaving policies, and the benchmarks run on CPU 0. We can see that the

Table 2. HPC workloads for evaluation. “BW” stands for “bandwidth”.

	Type	Workload Characterization	Input Problem	Mem. footprint	BW-hungry Objects
BT	Dense linear algebra	Unit-strided memory accesses from dense matrices	Class E	166 GB	u, rsh, forcing
LU	Sparse linear algebra	Indexed loads and stores from compressed matrices	Class E	134 GB	u, rsd
CG	Sparse linear algebra	Irregular memory accesses based on indirect indexing	Class E	134 GB	a
MG	Structured grids	Dynamic updates based on subdivided regular grids	Class E	210 GB	v, r
SP	Structured grids	Intense floating-point computations for linear equations	Class E	174 GB	u, rsh, forcing
FT	Spectral method	Bandwidth-consuming matrix transpose	Class D	80 GB	u0, u1
XSbench	Monte Carlo	Computation based on repeated random trials	Extra large	116 GB	nuclide_grids

performance difference between the interleaving RDRAM+CXL and interleaving LDRAM+CXL is less than 9.2% for all benchmark. In other words, *interleaving CXL and RDRAM, we do not need local fast memory to achieve a similar performance.*

The above results are because of large performance gap between the CXL memory and DDR (e.g., $2.1\times$ and $1.2\times$ longer in memory access latency, compared to LDRAM and RDRAM respectively.): because of data dependency and limited hardware resources (e.g., MSHR and the queues in MC), the performance is highly impacted by the slow CXL memory and irrelevant whether the LDRAM or RDRAM is utilized.

HPC observation 4. The CXL memory can show unexpected high performance for the latency-sensitive applications with random memory accesses.

The CG results in Figures 6 and 7 support the above observation. CG is a latency-sensitive application because of its indirect indexing-based memory accesses. In Figure 6, CXL preferred performs better than RDRAM preferred by 10.9%-57.2% when the number of threads is 4-20. This seems to be counter-intuitive, because the CXL memory has higher latency than RDRAM. We think that this superior performance may come from the optimization in the CXL device or customized caching policy in the processor for expensive, CPU-less memory accesses [49], and this optimization is especially effective for CG-style workloads. When the number of threads is larger than 20, the CXL memory accesses become more intensive, and inferior performance of the CXL memory becomes more obvious.

In Figure 7, we also observe that CXL preferred outperforms any other CXL-related interleaving policies in CG, despite other policies provide higher bandwidth and shorter average access-latency. This indicates that for a latency-sensitive workload with a random, scattered memory accesses, gathering accesses in one memory node instead of spreading to multiple memory nodes benefits performance because of reduction of row buffer misses in memory devices.

4.2 Object-Level Interleaving

Instead of generally interleaving pages at the application level (named *application-level interleaving*), we propose a method to interleave pages at the data object level. This enables fine-grained control over how pages are interleaved. Since different data objects have different access patterns, using the fine-grained control allows the bandwidth-sensitive object to be accessed with high bandwidth, while the latency-sensitive object is allocated locally for high performance.

Interleaving method. We use two criteria to select data objects and allocate them using the interleaving policy.

- The object must have a large memory footprint, which means taking at least 10% of total memory consumption.
- Memory accesses to the object must be intensive; among the data objects that meet the first criterion, we select data objects with the largest number of memory accesses. Multiple data objects may be selected.

With high thread-level parallelism, memory accesses to the above data objects are more sensitive to memory bandwidth. Besides the above data objects, the memory allocation for other objects uses the “preferred” policy. The last column in Table 2 summarizes those bandwidth-hungry data objects selected for interleaving.

We evaluate the effectiveness of our object-level interleaving using the following approach. In each test, we run the workload on CPU 0 using both LDRAM (memory node 0) and CXL memory. The LDRAM is either 64GB or 128GB, and the memory consumption of all applications exceeding 64GB, which allows us to assess the cases with both sufficient and insufficient LDRAM. The CXL memory is consistently 128GB. We make the following object-level interleaving observations (abbreviated as OLI observations).

OLI observation 1. When the local DRAM is sufficient (with 128 GB), the object-level interleaving performance is similar to that with LDRAM preferred, and consistently outperforms the application-level interleaving in all scenarios.

Figure 8 shows that OLI performance is 65% better than the application-level interleaving on average, demonstrating the effectiveness of OLI to meet the diverse requirements of latency-sensitive and bandwidth-sensitive objects. Additionally, *we observe that by using OLI, we can effectively reduce the fast memory size by an average of 48% (and up to 80% for FT), while still achieving similar performance as LDRAM preferred.* The performance difference between OLI and LDRAM preferred is less than 1% on average for all HPC workloads, except XSbench, when LDRAM is sufficient.

OLI observation 2. When the local DRAM is insufficient (64 GB), the OLI outperforms any other cases.

Figure 9 shows that on average, OLI performs $1.42\times$ better than LDRAM preferred (and up to $2.35\times$ for BT). It also outperforms the application-level interleaving by $1.32\times$ on average (and up to $1.84\times$ for LU). This is because of the following reasons. (1) The performance of LDRAM preferred

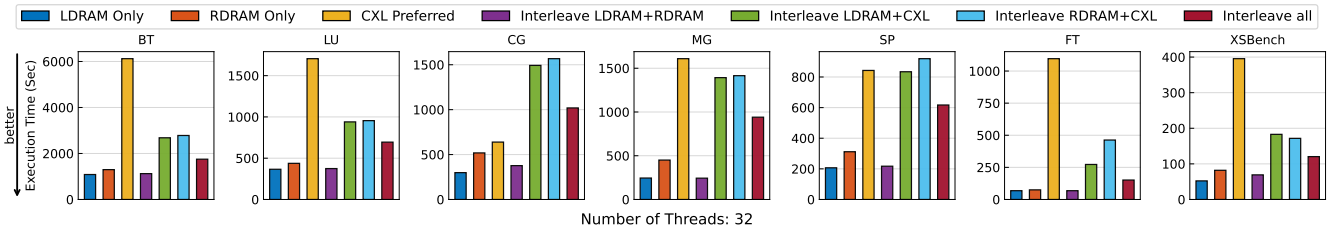


Figure 7. The performance of various interleaving policies for HPC applications.

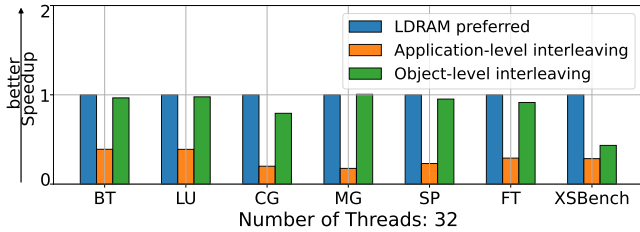


Figure 8. Performance speedup of various memory allocation strategies compared to “LDRAM preferred”, using sufficient LDRAM (128GB).

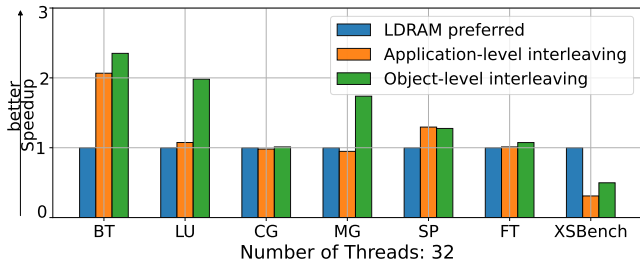


Figure 9. Performance speedup of various memory allocation strategies, compared to “LDRAM preferred”, using insufficient LDRAM (64GB).

is highly related to when the data objects are allocated. If LDRAM is full, latency-sensitive objects might end up in the slower CXL memory. (2) The bandwidth-sensitive data objects do not have opportunities to be allocated on both LDRAM and CXL for high bandwidth.

In XSBench, LDRAM preferred performs better than both application-level and object-level interleaving. This is because most of the memory accesses in XSBench are concentrated in a small, latency-sensitive memory set.

Takeaway: the CXL memory offers additional bandwidth, but HPC workloads may not benefit from it directly. The application-level interleaving can undermine performance, while the data object-level interleaving delivers performance comparable to or better than the default LDRAM-centric page allocation while saving fast memory size.

5 CXL for Large Language Models

LLMs are crucial for powering various AI applications, but their substantial memory footprint presents deployment

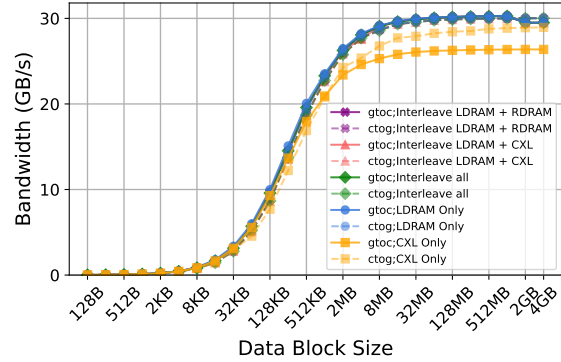


Figure 10. Data transfer bandwidth between the GPU (labeled as “g”) and CPU (labeled as “c”).

challenges. We study the performance of LLMs with *tensor offloading* techniques using the CXL memory, a promising solution to address the constraint of GPU memory capacity. Tensor offloading moves tensors out of GPU memory when they are not in use, allowing for the execution of larger models that exceed the GPU’s memory capacity. The evaluation is conducted on the system A, featuring an NVIDIA A10 GPU with 24GB memory, connected to the host CPU via PCIe Gen 4, offering a maximum bandwidth of 32GB/s.

The CXL memory on the system A uses CXL 1.1, which does not allow the GPU to directly access the CXL memory; instead, the accesses must go through the CPU. Under CXL 1.1, the data path from the GPU to the CXL memory is “GPU - PCIe - CPU - PCIe - CXL memory”, longer than the direct “CPU - PCIe - CXL memory” path. The data path in CXL 1.1 is different from the CXL devices peer-to-peer access supported in CXL 3.1 (using “GPU - PCIe - CXL memory”). We explore the effects of the CXL 1.1 data path on the data transfer bandwidth and latency.

Bandwidth results. We measure memory access bandwidth by repeatedly and randomly copying data blocks between the GPU memory (labeled as “g”) and CPU memory (labeled as “c”) using various page allocation strategies. The size of the data blocks varies from 128 byte to 4GB, illustrated in Figure 10. We use membind [4] to specify the memory device as the source or destination for data transfers.

LLM basic observation 1. The memory bandwidth for the GPU access to the memory hierarchy with CXL is constrained

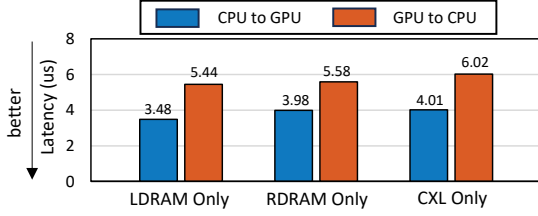


Figure 11. Data transfer latency between the GPU and CPU. The data size is 64 bytes.

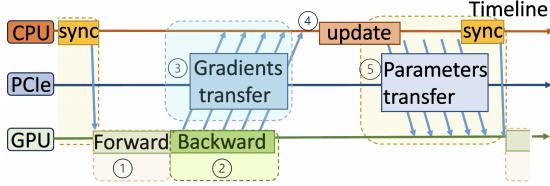


Figure 12. Overview of ZeRO-Offload in a training step.

by the PCIe bandwidth between the CPU and GPU, due to the absence of peer-to-peer access support in CXL 1.1.

Counter-intuitively, using the CXL memory does not increase memory bandwidth for the GPU. As shown in Figure 10, the peak memory bandwidth is similar across various memory interleaving policies (the difference is less than 3%). This lack of bandwidth increase with the CXL memory is primarily due to the PCIe interconnect between the CPU and GPU acting as a performance bottleneck.

Latency results. We develop a microbenchmark to measure the data transfer latency. The microbenchmark runs on CPU 1 (the CPU close to the CXL memory) and uses `cudaMemcpy()` for data transfer. The benchmark repeatedly transfers a 64-byte data (a cache block) between the CPU and GPU. The transfer happens 100K times, and we report average time for one transfer. We use `membind`, similar to the bandwidth tests. Figure 11 shows the results.

LLM basic observation 2. Accessing the CXL memory from the GPU can result in longer latency than expected.

The difference of data transfer latency between “GPU - CXL memory” and “GPU - CPU memory” is greater than the latency difference between “CPU - CXL memory” and “CPU - CPU memory”, shown in Figure 11. For example, accessing the CXL memory from the GPU is, on average, 500 ns longer than accessing the CPU memory from the GPU. In contrast, accessing the CXL memory from the CPU is only 120 ns longer than accessing the CPU memory from the CPU. The longer latency-difference from the GPU side comes from the longer data-path between the GPU and CXL memory.

We study the implication of using the CXL memory for LLM using tensor offloading, as follows.

5.1 LLM Training

5.1.1 ZeRO-Offload Background. ZeRO-Offload is a commonly employed in the industry to enable larger LLM training using smaller GPU memory. To save the GPU memory,

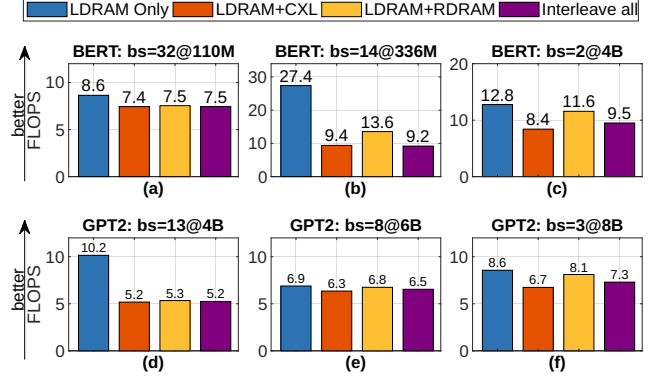


Figure 13. Performance with various interleaving policies and model sizes for BERT and GPT2.

ZeRO-Offload efficiently offloads full-precision model parameters, gradients, and optimizer states (e.g., momentum and variance) to the CPU memory, moving them back to GPU memory when needed. Figure 12 depicts the workflow of ZeRO-Offload. Specifically, it ① performs forward and ② backward computation on GPU; and ③ offloads gradients to the CPU memory during the backward step. To reduce the overhead of tensor movement between CPU and GPU ④, ZeRO-Offload performs optimization computation (e.g., the ADAM optimizer) on the CPU; and ⑤ moves updated parameters from the CPU memory to the GPU memory before the next forward step. This strategy minimizes data movement volume between the GPU and CPU memory for each training step. As a result, ZeRO-Offload enables 10× larger model training on a single GPU with 1.4× higher throughput.

5.1.2 Using CXL Memory. We evaluate two LLMs: BERT [11] and GPT2 [36]. For BERT, we consider three configurations: 110 million (base), 340 million (medium), and 4 billion (large) parameters. For GPT2, we evaluate models with 4, 6, and 8 billion parameters. Figures 13 shows the performance with various interleaving policies and model sizes. We use the notation “bs=effective batch size@model size” to represent the batch size and number of model parameters. For a given model size, the batch size is chosen to be the maximum without causing an out-of-memory (OOM) error on the GPU. To better understand the performance, we break it down to the “optimization step” (i.e., the ADAM optimizer on the CPU, which is exposed to the critical path) and “data movement” (i.e., the gradient transfer from the GPU to the CPU and the parameter transfer from the CPU to the GPU). The memory capacities for various interleaving policies (i.e., LDRAM only, LDRAM+CXL, LDRAM+RDRAM, and “interleave all”) are 196GB, 324GB, 392GB, and 520GB. Figures 14 shows the results, including the data movement exposed to the critical path.

Evaluation results. LLM training observation 1. Using the CXL memory bring little performance improvement or even negative performance impact to ZeRO-Offloading.

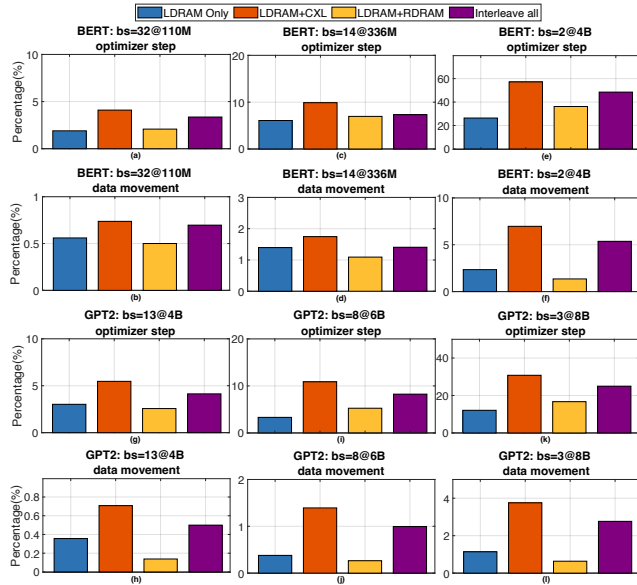


Figure 14. Performance of the optimizer and data movement in BERT and GPT2 under various interleaving policies. The percentage numbers are in terms of total training time.

Take GPT2 as an example. Figure 13 shows that the performance difference between LDRAM+RDRAM, LDRAM+CXL, and “interleave all” is less than 5% for the 4B and 6B models. For the 8B model, LDRAM outperforms “interleave all” by 14%, and LDRAM+RDRAM outperforms LDRAM+CXL by 16%. There is no performance benefit of using CXL.

Figure 14 reveals three reasons for the above observation. (1) The data movement takes a rather small portion of the training time in GPT2 (less than 5% in all cases). (2) Because of the bottleneck in the extra PCIe, the data movement does not get benefits from the better bandwidth offered by interleaving CXL and DDR (the CPU memory). Instead, the data movement suffers from longer access latency of the CXL memory. As a result, compared with using LDRAM, using CXL actually increases data transfer time and has a minor impact on the training time. (3) The optimizer takes a larger portion of the training time, compared to the data movement. The optimizer happens on the CPU and is sensitive to memory latency. Using CXL increases its execution time (2%-18%), compared to using LDRAM. When the batch size is small, the optimizer takes a significant portion of the training time (e.g., 31% when $bs=3@8B$). In such cases, optimizer slowdown substantially decreases overall training throughput. For example, when $bs=3@8B$, using “interleave all” performs worse than LDRAM+RDRAM by 11% due to the worse performance in the optimizer by 8%. We have the similar observations for BERT.

We expect that using a larger model (such as GPT-3 with 175 billion parameters) would result in data movement taking a larger portion of the training time. Unfortunately, we cannot evaluate such a large model because of the limited

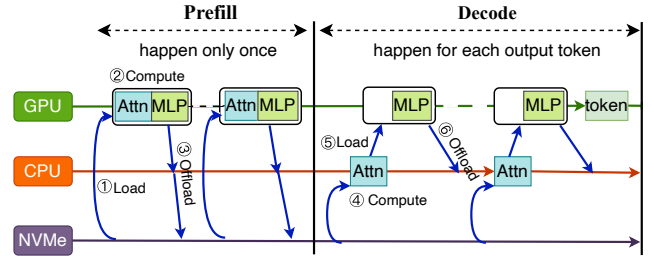


Figure 15. Overview of LLM inference with FlexGen.

memory capacity in our GPU. In addition, after reducing the data path between the GPU and CXL memory, the CXL memory can play a bigger role in reducing training time. Also, using the interleaving policy for the optimizer is not good for performance because of the latency sensitive nature of the optimizer. Using the first touch or “preferred policy”, the optimizer performance can be improved.

5.2 LLM Inference

5.2.1 FlexGen Background. LLM inference is memory-consuming. FlexGen [46] is a cutting-edge framework designed for LLM *inference* with constrained GPU memory capacity. To address the memory capacity limitation, FlexGen offloads model parameters, KV cache, and activations to the host CPU memory hierarchy (including DRAM and NVMe SSD). Figure 15 shows the workflow of FlexGen. The LLM inference consists of two stages: *prefill* and *decode*.

During the *prefill stage*, which happens only once per inference batch, (1) FlexGen transfers parameters from the CPU memory hierarchy to the GPU. (2) FlexGen executes attention and MLP computation layer by layer on the GPU. (3) At the end of each attention layer, the generated KV cache is offloaded to the CPU memory hierarchy. The *decode stage* generates tokens and significantly influences the overall throughput of the inference process. To minimize tensor movement between the GPU and CPU, (4) FlexGen conducts attention computation directly on the CPU. (5) FlexGen then transfers model parameters and activations generated in the attention layer from the CPU to the GPU for MLP computation, and (6) transfers activations generated in the MLP layer to the CPU for the following computation.

Offloading policy and cost model. FlexGen allows tensors to be partially placed in the CPU memory hierarchy and uses a cost model to determine the optimal offloading policy for maximum inference throughput within a memory capacity constraint. The cost model considers latency and bandwidth differences between NVMe and DRAM but does not differentiate among LDRAM, RDRAM, and CXL memory.

5.2.2 Using CXL Memory. Evaluation setup. We evaluate LLaMA [50] with 65 billion parameters and OPT [66] with 66 billion parameters. The lengths of the input prompts and output tokens are standardized at 2,048 and 256, respectively. The evaluation platform has 196 GB LDRAM, 196 GB

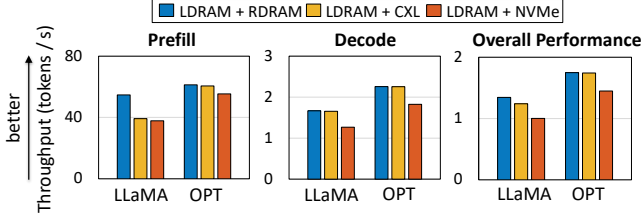


Figure 16. Comparison LLM inference throughput across memory systems, each with 324 GB capacity.

RDRAM, 128 GB CXL, and 128 GB NVMe. Leveraging GRUB mmap and numactl [4], we build the CPU memory hierarchy with various capacities and media types.

Evaluation results. LLM inference observation (LIO) 1. The performance of the CXL memory is comparable to that of RDRAM, and surpasses NVMe when applied in LLM inference with the tensor offloading.

Figure 16 presents the results. Each evaluation uses two equal-sized memory medias with a total capacity of 324 GB. According to FlexGen’s tensor offloading policy, only 8% of the KV cache resides on the GPU, and the remaining KV cache, weights, and activations reside on the CPU. Figure 16 shows that the inference throughput using LDRAM + CXL is similar to that of LDRAM + RDRAM, with the difference being less than 3%. Furthermore, LDRAM + CXL shows an improvement of 24% for LLaMA and 20% for OPT in overall throughput, compared to LDRAM + NVMe.

LIO 2. The throughput of prefill and decode stages responds differently to memory latency and bandwidth.

Figure 16 shows that during the prefill stage, the throughput difference in the prefill stage across the three interleaving policies largely reflects the trend of latency difference in the memory systems. For example, LDRAM + RDRAM outperforms LDRAM + CXL and LDRAM + NVMe by 20% and 28% on average, respectively. This is because during the prefill stage, tensors are loaded from the CPU to the GPU and such data loading is sensitive to the latency.

In contrast, during the decode stage, the throughput is more sensitive to memory bandwidth (see Figure 16). The decoding throughput using LDRAM + CXL is 27% better than using LDRAM + NVMe on average. LDRAM + RDRAM and LDRAM + CXL perform similarly. This is because in the decode stage, the attention computation happens on the CPU, leading to intensive data access and sensitive to large bandwidth difference between CXL and NVMe (but not relatively small difference between CXL and RDRAM).

LIO 3. CXL increases the capacity of the memory system, thereby enhancing the throughput of LLM inference due to larger batch size.

Figure 17 illustrates the inference throughput with various capacities of the CPU memory. Table 3 summarizes the offloading policy search results with those capacities. The LLM batch size scales up with the increased memory

Table 3. LLM inference configuration for evaluation. “BS” and “c” stands for “batch size” and “KV cache”, respectively. According to offloading policy in FlexGen, all weights and activations are stored in CPU memory.

LLM	Memory hierarchy	BS	c on GPU	c on CPU	Memory footprint
LLaMA	LDRAM Only (196 GB)	14	20%	80%	200 GB
LLaMA	LDRAM + RDRAM (392 GB)	40	4%	96%	348 GB
LLaMA	Interleave all (520 GB)	56	4%	96%	438 GB
OPT	LDRAM Only (196 GB)	9	27%	73%	168 GB
OPT	LDRAM + RDRAM (392 GB)	40	4%	96%	326 GB
OPT	Interleave all (520 GB)	64	4%	96%	448 GB

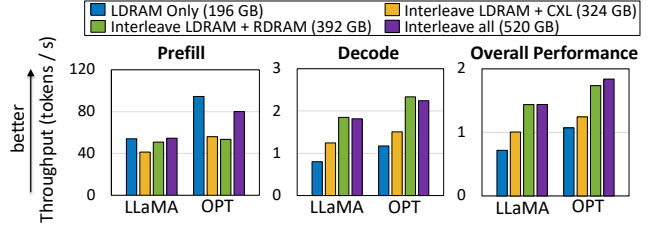


Figure 17. Comparison of LLM inference throughput across various memory systems with different capacities.

system capacity. Specifically, with LDRAM + CXL, LDRAM + RDRAM, and LDRAM + RDRAM + CXL, the batch size increases by 1.14 \times , 1.85 \times , and 3 \times for LLaMA, and 2.11 \times , 3.44 \times and 6.11 \times for OPT, respectively, compared to the case of utilizing LDRAM only. The overall throughput increases by 28%, 81% and 86% on average respectively, compared to LDRAM only.

We further decompose performance into prefill and decode. During the prefill stage, the inference throughput is dominated by the latency of GPU accessing the CPU memory hierarchy, hence LDRAM only outperforms LDRAM + CXL, LDRAM + RDRAM, and LDRAM + RDRAM + CXL by 50%, 41%, and 9% on average, respectively. However, during the decode stage, as the batch size increases, the inference throughput improves by 42%, 114%, and 109% on average for LDRAM + CXL, LDRAM + RDRAM, and LDRAM + RDRAM + CXL respectively, compared with LDRAM only.

Takeaway: (1) The CXL memory as a memory capacity expander enables LLMs to train and infer with larger batch sizes, which in turn improves system throughput. However, when the GPU accesses the CXL memory, the lack of peer-to-peer access support in CXL 1.1 prevents them from leveraging the extra bandwidth and results in longer latency due to the extended data path. (2) Computation of-floaded to the CPU can benefit from extra CXL bandwidth.

6 Memory Tiering based on Page Migration

Memory tiering is an application-transparent solution to integrate the CXL memory into the existing memory systems. Treating the CXL memory as a memory tier, existing memory tiering solutions [10, 24, 32, 37, 41, 53] rely on memory profiling to count memory accesses at the page level. Then,

those solutions move frequently accessed (hot) pages to the fast memory tier, and demote less frequently access (cold) pages to the slow memory tier. In contrast to the interleaving studied in Sections 4-5, which are static page placement solutions, the memory tiering solutions are dynamic.

We use the system A for evaluation. We limit the capacity of the fast memory tier (i.e., LDRAM) while the slow memory tier (i.e., CXL) has unlimited capacity. We evaluate three state-of-the-art memory tiering solutions as follows. We also evaluate No Balance (between NUMA nodes) representing the static page placement without migration. Our study is featured with analyzing the interplay between page migration and interleaving.

- AutoNUMA [10] tracks memory accesses by unmapping pages to generate hint faults, and periodically scans the application address space to find hint faults. AutoNUMA promotes pages using a NUMA-distance-based, *static* memory-access threshold to avoid unnecessary page migration. AutoNUMA is enabled by setting `numa_balancing` to 1 in `/proc/sys/kernel` (the default Linux setting).
- Tiering-0.8 [53] also uses hint faults to identify hot pages. Unlike AutoNUMA, Tiering-0.8 *dynamically* adjusts the promotion criteria to throttle migration traffic. It considers the recency of page accesses to decide page promotion and demotion. Tiering-0.8 is enabled by setting `numa_balancing` to 2, and it uses the Linux default promotion threshold for initialization.
- TPP [32] utilizes both hint faults and the active list in the OS to determine page migration, considering both access recency and page activeness for promotion.

6.1 Page Migration with Application-Level Interleaving

Evaluation setup. To study the impact of page migration, we evaluate four memory-intensive applications, including BTree [1], an in-memory index lookup; PageRank [6] and Graph500 [33], both graph processing applications; and Silo [52], an in-memory database engine. We run them with 64 threads. We configure the memory consumption of each application to be around 130GB. This configuration ensures a fair comparison between static page placement solutions (i.e., the NUMA first touch and interleaving): LDRAM (i.e., 50GB) is set to less than half of each application’s memory consumption, hence both solutions can fully utilize LDRAM.

Metrics. We report the execution time and page migration statistics, including the number of hint faults and migrated pages. Such statistics is collected by periodically reading the Linux counters from `/proc/vmstat`. Those counters capture page accesses from the entire system, but primarily influenced by page migrations because of the application.

Evaluation results. Page migration observation (PMO) 1. Different applications perform differently with different page

migration and static page placement solutions. No single solution can get the best performance for all applications.

Figure 18 shows the execution time. We observe that BTree is not sensitive to any solution (the performance variance is less than 3%), because of its highly irregular memory access patterns. PageRank achieves the best performance with the first touch without page migration, which is 88% better than any page migration solution plus the interleaving, because PageRank has a relatively small and stable set of hot pages. Graph500 achieves the best performance with Tiering-0.8 plus the interleaving, outperforming other solutions by up to 33%, because Graph500’s hot pages are scattered across memory tiers and the interleaving is helpful for improving data locality. Silo achieves the best performance with the Tiering-0.8 plus the first touch, outperforming other solutions by up to 20%. Different from Graph500 where the hot data is distributed to many pages, Silo’s hot data is gathered into fewer pages, making the first touch more effective than the interleaving.

PMO 2. When using first touch, Tiering-0.8 outperforms TPP and AutoNUMA for memory tiering.

Figure 18 illustrates that, using the first touch, Tiering-0.8 outperforms NO Balance, AutoNUMA, and TPP by 7%, 3%, and 31% on average, respectively. Table 4 reveals the reasons. Compared to TPP, Tiering-0.8 has $59 \times$ fewer hint faults on average. Memory profiling in TPP can incur a large overhead, and the reduced number of hint faults in Tiering-0.8 indicates less profiling overhead, contributing to performance improvement. Compared to AutoNUMA, Tiering-0.8 has a comparable number of hint faults but exhibits large variance in the number of migrated pages. For example, in PageRank, Tiering-0.8 results in 7.6 million more migrations than AutoNUMA. This variance is due to the dynamic adjustment of the page promotion threshold in Tiering-0.8.

PMO 3. The page migration based on hint faults is not integrated well with the application-level interleaving.

Table 4 reveals that using page migration plus the application level interleaving, the number of hint faults is $72,721 \times$ less than that of page migration plus the first touch on average. Our investigation reveals that when the application-level interleaving is employed, the application’s pages are placed in unmigratable regions, preventing the pages to trigger hint faults. Hence, the page migration cannot be effective.

6.2 Page Migration with Object-Level Interleaving

Evaluation setup. We evaluate HPC workloads listed in Table 2. To enable fair comparison between the application- and object-level interleaving, the capacity of LDRAM is set to 40GB for FT, 100GB for MG, and 50GB for others, such that all static page placement solutions can fully utilize LDRAM for each application. The CXL memory does not have a capacity constraint, because it is the slowest memory tier. We use 32 threads on the socket 1.

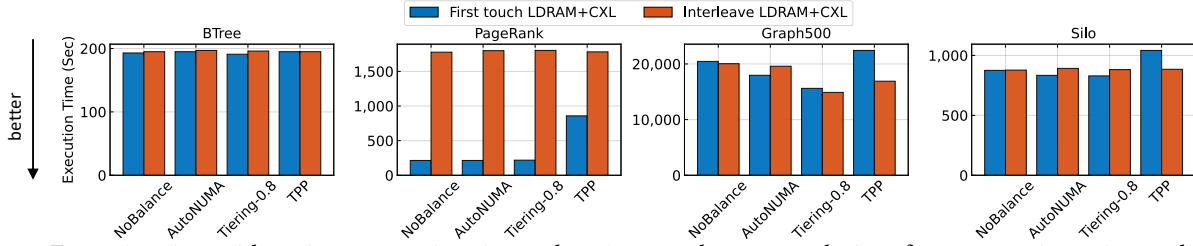


Figure 18. Execution time with various page migration and static page placement solutions for memory-intensive applications.

Table 4. NUMA statistics with various page migration and static page placement solutions.

		AutoNUMA		Tiering-0.8		TPP	
		hint_faults	migrated_pages	hint_faults	migrated_pages	hint_faults	migrated_pages
BTree	First touch	336,469,816	3	125,802,092	46	4,654,013,085	5
	Interleave	6,092	492	6,916	51	5,092	1
PageRank	First touch	31,793,182	117	63,893,091	7,653,699	5,894,907,183	6,929,247
	Interleave	28,398	10,050	613,906	4,412	165,721	15
Graph500	First touch	66,495,782	118,621	398,259,304	6,134	36,393,830,981	190
	Interleave	4,381,521	124	282,087	6,114	74,432,220	1,569
Silo	First touch	146,665,022	21,494	220,094,592	3,264	1,588,732,736	1,497,420
	Interleave	11,428	10	5,581,434	14,512	60,638	0

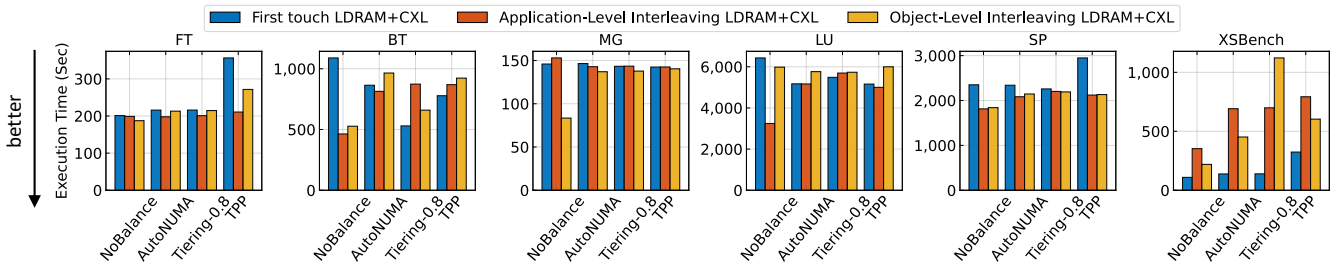


Figure 19. Execution time with various page management solutions for HPC applications.

Evaluation results. PMO 4. Using the page migration plus the object-level interleaving results in minor performance improvement on HPC workloads, compared to the object-level interleaving without page migration.

Figure 19 shows that *without the page migration*, the object-level interleaving outperforms both the first-touch and application-level interleaving by up to 45%. However, the page migration negatively impacts the effectiveness of the object-level interleaving: when using AutoNUMA, Tiering-0.8, and TPP, the performance degrades by 46%, 88%, and 63% on average respectively, compared to using the object-level interleaving without page migration. This occurs because the object-level interleaving utilizes the additional CXL bandwidth for bandwidth-hungry objects. However, the page migration undermines this benefit.

PMO 5. The page migration can improve performance for some applications but lose performance for others.

Figure 19 shows that different HPC workloads exhibit different preferences for page migration. For example, the page migration degrades performance for FT, SP and XSBench, and yields almost no performance difference in MG, regardless of using the interleaving or first touch, because these

workloads have uniformly accessed working set or highly skewed and scattered hot memory region, which make hotness detection challenging. In contrast, the page migration improves the performance of BT and LU by up to 51% and 20%, respectively, since hot pages in BT and LU have good temporal and spatial locality to be detected.

Takeaway: (1) There is significant potential to improve the performance of page migration in the memory tiering solutions. (2) Dynamic page migration and static page interleaving are not well-integrated. (3) Dynamic page migration may degrade performance; a better static page placement strategy *without page migration*, such as object-level interleaving, can lead to better performance.

7 Related Work

CXL. CXL has garnered significant attention from academia and industry [8, 13, 16, 27, 28, 32, 44, 45, 47, 49, 54, 63, 65]. For example, Google has explored the potential of the CXL memory in memory tiering and swapping in its cloud computing infrastructure [26], while Microsoft has developed CXL-based memory pools for public cloud platforms [7, 27].

Most of the explorations of using the CXL memory leverage NUMA servers to emulate CXL memory performance [13, 16, 63, 64]. For example, Yang et al. [63] overcome the memory wall with emulated CXL-enabled SSDs. There is also a surge in research focusing on specific applications of CXL memory [3, 7, 8, 16, 25, 28, 48]. Besides the above efforts, Sun et al. [49] demystify the CXL memory performance using genuine CXL-ready systems and devices, which is the first paper that explores the real CXL-ready systems. However, the vast of applications from other fields (such as HPC and AI) are not extensively studied, and memory tiering and its interplay with page interleaving are not studied.

Tiered memory system. Different memory components can show different memory latency, bandwidth, capacity, and monetary cost. Using multiple memory components, we can build a tiered memory systems to save cost and improve memory capacity [2, 9, 20, 23, 42, 61]. Using the CXL memory, it is natural to build a tiered memory where local DDR is the fast tier and the CXL memory is a slow tier. Many solutions [12, 14, 17, 18, 21, 29, 31, 37–39, 55, 57–59] have been proposed to explore and leverage the tiered memory systems to improve application performance. However, the performance of those solutions on CXL-ready systems (especially their interplay with page interleaving) is not clear [19, 43, 47].

8 Conclusions

We characterize the performance of the real CXL memory and explore its use cases. We study the performance of the CXL memory with a spectrum of HPC applications, explore the use of CXL for LLM training and inference, and investigate how application-transparent solutions (page interleaving and memory tiering) perform with the real CXL. We also create a data object-level interleaving method that switches between the interleaving and NUMA node-preferred policies at the data object level, and demonstrate its superior performance.

References

- [1] Reto Achermann and Ashish Panwar. 2019. Mitosis workload BTree. <https://github.com/mitosis-project/mitosis-workload-btree>.
- [2] Neha Agarwal and Thomas F. Wenisch. 2017. Thermostat: Application-transparent Page Management for Two-tiered Main Memory. *Proceedings of the Twenty-Second International Conference on Architectural Support for Programming Languages and Operating Systems* (2017). <https://api.semanticscholar.org/CorpusID:8753499>
- [3] Gustavo Alonso, Ana Klimovic, Tom Kuchler, and Michael Wawrzoniak. 2023. Rethinking Serverless Computing: from the Programming Model to the Platform Design. (2023).
- [4] Andi Kleen (SUSE Labs). [n. d.]. NUMA Support for Linux. <https://github.com/numactl/numactl>.
- [5] K. Asanovic, R. Bodik, B. Catanzaro, J. Gebis, P. Husbands, K. Keutzer, D. Patterson, W. Plishker, J. Shalf, S. Williams, and K. Yelick. 2006. *The Landscape of Parallel Computing Research: A View from Berkeley*. Technical Report UCB/EECS-2006-18. University of California at Berkeley.
- [6] Scott Beamer, Krste Asanović, and David Patterson. 2015. The GAP benchmark suite. *arXiv preprint arXiv:1508.03619* (2015).
- [7] Daniel S Berger, Daniel Ernst, Huaicheng Li, Pantea Zardoshti, Monish Shah, Samir Rajadnya, Scott Lee, Lisa Hsu, Ishwar Agarwal, Mark D Hill, et al. 2023. Design Tradeoffs in CXL-Based Memory Pools for Public Cloud Platforms. *IEEE Micro* 43, 2 (2023), 30–38.
- [8] Albert Cho, Anish Saxena, Moinuddin Qureshi, and Alexandros Daglis. 2023. A Case for CXL-Centric Server Processors. *arXiv preprint arXiv:2305.05033* (2023).
- [9] Jinyoung Choi, Sergey Blagodurov, and Hung-Wei Tseng. 2021. Dancing in the Dark: Profiling for Tiered Memory. *2021 IEEE International Parallel and Distributed Processing Symposium (IPDPS)* (2021), 13–22. <https://api.semanticscholar.org/CorpusID:232134240>
- [10] J. Corbet. [n. d.]. AutoNUMA: the Other Approach to NUMA Scheduling. <http://lwn.net/Articles/488709>.
- [11] Jacob Devlin, Ming-Wei Chang, Kenton Lee, and Kristina Toutanova. 2018. Bert: Pre-training of deep bidirectional transformers for language understanding. *arXiv preprint arXiv:1810.04805* (2018).
- [12] Subramanya R. Dulloor, Amitabha Roy, Zheguang Zhao, Narayanan Sundaram, Nadathur Satish, Rajesh Sankaran, Jeffrey R. Jackson, and Karsten Schwan. 2016. Data tiering in heterogeneous memory systems. *Proceedings of the Eleventh European Conference on Computer Systems* (2016). <https://api.semanticscholar.org/CorpusID:8681081>
- [13] Donghyun Gouk, Miryeong Kwon, Hanyeoreum Bae, Sangwon Lee, and Myoungsoo Jung. 2023. Memory pooling with cxl. *IEEE Micro* 43, 2 (2023), 48–57.
- [14] Mark Hildebrand, Jawad Ali Khan, Sanjeev N. Trika, Jason Lowe-Power, and Venkatesh Akella. 2020. AutoTM: Automatic Tensor Movement in Heterogeneous Memory Systems using Integer Linear Programming. *Proceedings of the Twenty-Fifth International Conference on Architectural Support for Programming Languages and Operating Systems* (2020). <https://api.semanticscholar.org/CorpusID:212641763>
- [15] Intel Corporation. 2019. Intel Memory Latency Checker v3.5. <https://software.intel.com/en-us/articles/intel-memory-latency-checker>
- [16] Junhyeok Jang, Hanjin Choi, Hanyeoreum Bae, Seungjun Lee, Miryeong Kwon, and Myoungsoo Jung. 2023. CXL-ANNS: Software-Hardware Collaborative Memory Disaggregation and Computation for Billion-Scale Approximate Nearest Neighbor Search. In *2023 USENIX Annual Technical Conference (USENIX ATC 23)*. USENIX Association, Boston, MA, 585–600. <https://www.usenix.org/conference/atc23/presentation/jang>
- [17] Sudarsun Kannan, Ada Gavrilovska, Vishal Gupta, and Karsten Schwan. 2017. HeteroOS — OS design for heterogeneous memory management in datacenter. *2017 ACM/IEEE 44th Annual International Symposium on Computer Architecture (ISCA)* (2017), 521–534. <https://api.semanticscholar.org/CorpusID:19189083>
- [18] Jonghyeon Kim, Wonkyo Choe, and Jeongseob Ahn. 2021. Exploring the Design Space of Page Management for Multi-Tiered Memory Systems. In *USENIX Annual Technical Conference*. <https://api.semanticscholar.org/CorpusID:236992513>
- [19] Kyung Duk Kim, Hyunseok Kim, Jinin So, Wonjae Lee, Jun-Hyeok Im, Sung-Rok Yoon and Sin-Chong Park, Jeonghyeon Cho, and Ho Uk Song. 2023. SMT: Software-Defined Memory Tiering for Heterogeneous Computing Systems With CXL Memory Expander. *IEEE Micro* 43 (2023), 20–29. <https://api.semanticscholar.org/CorpusID:256491961>
- [20] Vamsee Reddy Kommareddy, Clayton Hughes, Simon David Hammond, and Amro Awad. 2020. DeACT: Architecture-Aware Virtual Memory Support for Fabric Attached Memory Systems. *IEEE International Symposium on High-Performance Computer Architecture (HPCA)* (2020).
- [21] Sandeep Kumar, Aravinda Prasad, Smruti Ranjan Sarangi, and Sreenivas Subramoney. 2021. Radiant: efficient page table management for tiered memory systems. *Proceedings of the 2021 ACM SIGPLAN International Symposium on Memory Management* (2021). <https://>

- //api.semanticscholar.org/CorpusID:235463147
- [22] Astera Labs. [n. d.]. Breaking Through the Memory Wall. <https://www.asteralabs.com/general/breaking-through-the-memory-wall/>.
- [23] Taehyung Lee and Young Ik Eom. 2022. Optimizing the Page Hotness Measurement with Re-Fault Latency for Tiered Memory Systems. *2022 IEEE International Conference on Big Data and Smart Computing (BigComp) (2022)*, 275–279. <https://api.semanticscholar.org/CorpusID:247618508>
- [24] Taehyung Lee, Sumit Kumar Monga, Changwoo Min, and Young Ik Eom. 2023. MEMTIS: Efficient Memory Tiering with Dynamic Page Classification and Page Size Determination. In *Proceedings of the 29th Symposium on Operating Systems Principles*.
- [25] Alberto Lerner and Gustavo Alonso. 2024. CXL and the Return of Scale-Up Database Engines. *arXiv preprint arXiv:2401.01150 (2024)*.
- [26] Philip Levis, Kun Lin, and Amy Tai. 2023. A Case Against CXL Memory Pooling. In *Proceedings of the 22nd ACM Workshop on Hot Topics in Networks*. 18–24.
- [27] Huaicheng Li, Daniel S Berger, Lisa Hsu, Daniel Ernst, Pantea Zardoshti, Stanko Novakovic, Monish Shah, Samir Rajadnya, Scott Lee, Ishwar Agarwal, et al. 2023. Pond: CXL-based memory pooling systems for cloud platforms. In *Proceedings of the 28th ACM International Conference on Architectural Support for Programming Languages and Operating Systems, Volume 2*. 574–587.
- [28] Yuze Li and Shunyu Yao. 2023. Understanding and Optimizing Serverless Workloads in CXL-Enabled Tiered Memory. *arXiv preprint arXiv:2309.01736 (2023)*.
- [29] Zhe Li and Mingyu Wu. 2022. Transparent and lightweight object placement for managed workloads atop hybrid memories. *Proceedings of the 18th ACM SIGPLAN/SIGOPS International Conference on Virtual Execution Environments (2022)*. <https://api.semanticscholar.org/CorpusID:247108266>
- [30] Júnior Löff, Dalvan Griebler, Gabriele Mencagli, Gabriell Araujo, Massimo Torquati, Marco Danelutto, and Luiz Gustavo Fernandes. 2021. The NAS Parallel Benchmarks for evaluating C++ parallel programming frameworks on shared-memory architectures. *Future Generation Computer Systems* 125 (2021), 743–757. <https://doi.org/10.1016/j.future.2021.07.021>
- [31] Adnan Maruf, Ashikee Ghosh, Janki Bhimani, Daniela Campello, Andy Rudoff, and Raju Rangaswami. 2022. MULTI-CLOCK: Dynamic Tiering for Hybrid Memory Systems. *2022 IEEE International Symposium on High-Performance Computer Architecture (HPCA) (2022)*, 925–937. <https://api.semanticscholar.org/CorpusID:248865268>
- [32] Hasan Al Maruf, Hao Wang, Abhishek Dhanotia, Johannes Weiner, Niket Agarwal, Pallab Bhattacharya, Chris Petersen, Mosharaf Chowdhury, Shobhit Kanaujia, and Prakash Chauhan. 2023. TPP: Transparent Page Placement for CXL-Enabled Tiered-Memory. In *International Conference on Architectural Support for Programming Languages and Operating Systems (ASPLOS)*.
- [33] Richard C Murphy, Kyle B Wheeler, Brian W Barrett, and James A Ang. 2010. Introducing the graph 500. *Cray Users Group (CUG)* 19, 45–74 (2010), 22.
- [34] Vinicius Petrucci, Eishan Mirakhur, Nikesh Agarwal, Su Wei Lim, Vishal Tanna, Rita Gupta, and Mahesh Wagh. 2024. CXL Memory Expansion: A Closer Look on Actual Platform. <https://www.micron.com/content/dam/micron/global/public/products/white-paper/cxl-memory-expansion-a-close-look-on-actual-platform.pdf>.
- [35] Jonathan Prout. [n. d.]. Expanding Beyond Limits With CXL-based Memory. https://memverge.com/wp-content/uploads/2022/08/CXL-Forum_Samsung.pdf.
- [36] Alec Radford, Jeffrey Wu, Rewon Child, David Luan, Dario Amodei, Ilya Sutskever, et al. 2019. Language models are unsupervised multi-task learners. *OpenAI blog* 1, 8 (2019), 9.
- [37] Amanda Raybuck, Tim Stamler, Wei Zhang, Mattan Erez, and Simon Peter. 2021. HeMem: Scalable Tiered Memory Management for Big Data Applications and Real NVM. *Proceedings of the ACM SIGOPS 28th Symposium on Operating Systems Principles (2021)*. <https://api.semanticscholar.org/CorpusID:239029009>
- [38] Jie Ren, Jiaolin Luo, Ivy Peng, Kai Wu, and Dong Li. 2021. Optimizing Large-Scale Plasma Simulations on Persistent Memory-based Heterogeneous Memory with Effective Data Placement Across Memory Hierarchy. In *International Conference on Supercomputing (ICS)*.
- [39] Jie Ren, Jiaolin Luo, Kai Wu, Minjia Zhang, and Hyeran Jeon. 2021. Sentinel: Efficient Tensor Migration and Allocation on Heterogeneous Memory Systems for Deep Learning. *2021 IEEE International Symposium on High-Performance Computer Architecture (HPCA) (2021)*, 598–611. <https://api.semanticscholar.org/CorpusID:231620477>
- [40] Jie Ren, Samyam Rajbhandari, Reza Yazdani Aminabadi, Olatunji Ruwase, Shuangyan Yang, Minjia Zhang, Dong Li, and Yuxiong He. 2021. ZeRO-Offload: Democratizing Billion-Scale Model Training. In *USENIX Annual Technical Conference*.
- [41] Jie Ren, Dong Xu, Junhee Ryu, Kwangsik Shin, Daewoo Kim, and Dong Li. 2024. MTM: Rethinking Memory Profiling and Migration for Multi-Tiered Large Memory. In *Proceedings of the Nineteenth European Conference on Computer Systems (EuroSys)*.
- [42] Jee Ho Ryoo, Lizy Kurian John, and Arkaprava Basu. 2018. A Case for Granularity Aware Page Migration. *Proceedings of the 2018 International Conference on Supercomputing (2018)*. <https://api.semanticscholar.org/CorpusID:52277753>
- [43] Seokhyun Ryu, Sohyun Kim, Jaeyung Jun, Donguk Moon, Kyungsoo Lee, Jungmin Choi, Sunwoong Kim, Hyungsoo Kim, Luke Kim, Won Ha Choi, Moohyeon Nam, Dooyoung Hwang, Hongchan Roh, and Young-Pyo Joo. 2023. System Optimization of Data Analytics Platforms using Compute Express Link (CXL) Memory. *2023 IEEE International Conference on Big Data and Smart Computing (BigComp) (2023)*, 9–12. <https://api.semanticscholar.org/CorpusID:257644666>
- [44] Yizhou Shan, Will Lin, Zhiyuan Guo, and Yiyang Zhang. 2022. Towards a fully disaggregated and programmable data center. In *Proceedings of the 13th ACM SIGOPS Asia-Pacific Workshop on Systems*. 18–28.
- [45] Debendra Das Sharma, Robert Blankenship, and Daniel S. Berger. 2023. An Introduction to the Compute Express Link (CXL) Interconnect. [arXiv:2306.11227 \[cs.AR\]](https://arxiv.org/abs/2306.11227)
- [46] Ying Sheng, Lianmin Zheng, Binhang Yuan, Zhuohan Li, Max Ryabinin, Beidi Chen, Percy Liang, Christopher Ré, Ion Stoica, and Ce Zhang. 2023. FlexGen: High-Throughput Generative Inference of Large Language Models with a Single GPU. In *Proceedings of the 40th International Conference on Machine Learning (Honolulu, Hawaii, USA) (ICML '23)*. JMLR.org, Article 1288, 23 pages.
- [47] Joonseop Sim, Soohong Ahn, Taeyoung Ahn, Seungyong Lee, Myunghyun Rhee, Jooyoung Kim, Kwangsik Shin, Donguk Moon, Euisook Kim, and Kyoung Park. 2023. Computational CXL-Memory Solution for Accelerating Memory-Intensive Applications. *IEEE Computer Architecture Letters* 22 (2023), 5–8. <https://api.semanticscholar.org/CorpusID:254301130>
- [48] Kevin Song, Jiacheng Yang, Sihang Liu, and Gennady Pekhimenko. 2023. Lightweight Frequency-Based Tiering for CXL Memory Systems. *arXiv preprint arXiv:2312.04789 (2023)*.
- [49] Yan Sun, Yifan Yuan, Zeduo Yu, Reese Kuper, Chihun Song, Jinghan Huang, Houxiang Ji, Siddharth Agarwal, Jiaqi Lou, Ipoom Jeong, Ren Wang, Jung Ho Ahn, Tianyin Xu, and Nam Sung Kim. 2023. Demystifying CXL Memory with Genuine CXL-Ready Systems and Devices. In *IEEE/ACM International Symposium on Microarchitecture*.
- [50] Hugo Touvron, Thibaut Lavril, Gautier Izacard, Xavier Martinet, Marie-Anne Lachaux, Timothée Lacroix, Baptiste Rozière, Naman Goyal, Eric Hambro, Faisal Azhar, et al. 2023. Llama: Open and efficient foundation language models. *arXiv preprint arXiv:2302.13971 (2023)*.

- [51] John R Tramm, Andrew R Siegel, Tanzima Islam, and Martin Schulz. 2014. XSBench-the development and verification of a performance abstraction for Monte Carlo reactor analysis. *The Role of Reactor Physics toward a Sustainable Future (PHYSOR)* (2014).
- [52] Stephen Tu, Wenting Zheng, Eddie Kohler, Barbara Liskov, and Samuel Madden. 2013. Speedy transactions in multicore in-memory databases. In *Proceedings of the Twenty-Fourth ACM Symposium on Operating Systems Principles*. 18–32.
- [53] Vishal Verma. 2022. Tiering-0.8. <https://git.kernel.org/pub/scm/linux/kernel/git/vishal/tiering.git/log/?h=tiering-0.8>.
- [54] Jacob Wahlgren, Maya Gokhale, and Ivy B Peng. 2022. Evaluating Emerging CXL-enabled Memory Pooling for HPC Systems. In *2022 IEEE/ACM Workshop on Memory Centric High Performance Computing (MCHPC)*. IEEE, 11–20.
- [55] Chenxi Wang, Huimin Cui, Ting Cao, John N. Zigman, Haris Volos, Onur Mutlu, Fang Lv, Xiaobing Feng, and Guoqing Harry Xu. 2019. Panthera: holistic memory management for big data processing over hybrid memories. *Proceedings of the 40th ACM SIGPLAN Conference on Programming Language Design and Implementation* (2019). <https://api.semanticscholar.org/CorpusID:150372592>
- [56] Zixuan Wang, Xiao Liu, Jian Yang, Theodore Michailidis, Steven Swanson, and Jishen Zhao. 2020. Characterizing and modeling non-volatile memory systems. In *2020 53rd Annual IEEE/ACM International Symposium on Microarchitecture (MICRO)*. IEEE, 496–508.
- [57] Johannes Weiner, Niket Agarwal, Dan Schatzberg, Leon Yang, Hao Wang, Blaise Sanouillet, Bikash Sharma, Tejun Heo, M. Jain, Chunqiang Tang, and Dimitrios Skarlatos. 2022. TMO: transparent memory offloading in datacenters. *Proceedings of the 27th ACM International Conference on Architectural Support for Programming Languages and Operating Systems* (2022). <https://api.semanticscholar.org/CorpusID:247026540>
- [58] K. Wu, Y. Huang, and D. Li. 2017. Unimem: Runtime Data Management on Non-Volatile Memory-based Heterogeneous Main Memory. In *International Conference for High Performance Computing, Networking, Storage and Analysis*.
- [59] Kai Wu, Jie Ren, and Dong Li. 2018. Runtime Data Management on Non-Volatile Memory-Based Heterogeneous Memory for Task Parallel Programs. In *ACM/IEEE International Conference for High Performance Computing, Networking, Storage and Analysis*.
- [60] Lingfeng Xiang, Xingsheng Zhao, Jia Rao, Song Jiang, and Hong Jiang. 2022. Characterizing the performance of intel optane persistent memory: a close look at its on-dimm buffering. In *Proceedings of the Seventeenth European Conference on Computer Systems*. 488–505.
- [61] Zi Yan, Daniel Lustig, David W. Nellans, and Abhishek Bhattacharjee. 2019. Nimble Page Management for Tiered Memory Systems. *Proceedings of the Twenty-Fourth International Conference on Architectural Support for Programming Languages and Operating Systems* (2019). <https://api.semanticscholar.org/CorpusID:102348046>
- [62] Jian Yang, Juno Kim, Morteza Hoseinzadeh, Joseph Izraelevitz, and Steve Swanson. 2020. An empirical guide to the behavior and use of scalable persistent memory. In *18th USENIX Conference on File and Storage Technologies (FAST 20)*. 169–182.
- [63] Shao-Peng Yang, Minjae Kim, Sanghyun Nam, Juhyung Park, Jin yong Choi, Eeye Hyun Nam, Eunji Lee, Sungjin Lee, and Bryan S. Kim. 2023. Overcoming the Memory Wall with CXL-Enabled SSDs. In *2023 USENIX Annual Technical Conference (USENIX ATC 23)*. USENIX Association, Boston, MA, 601–617. <https://www.usenix.org/conference/atc23/presentation/yang-shao-peng>
- [64] Yiwei Yang, Pooneh Safayenikoo, Jiacheng Ma, Tanvir Ahmed Khan, and Andrew Quinn. 2023. CXLMemSim: A pure software simulated CXL. mem for performance characterization. *arXiv preprint arXiv:2303.06153* (2023).
- [65] Mingxing Zhang, Teng Ma, Jinqi Hua, Zheng Liu, Kang Chen, Ning Ding, Fan Du, Jinlei Jiang, Tao Ma, and Yongwei Wu. 2023. Partial Failure Resilient Memory Management System for (CXL-based) Distributed Shared Memory. In *Proceedings of the 29th Symposium on Operating Systems Principles*. 658–674.
- [66] Susan Zhang, Stephen Roller, Naman Goyal, Mikel Artetxe, Moya Chen, Shuohui Chen, Christopher Dewan, Mona Diab, Xian Li, Xi Victoria Lin, et al. 2022. Opt: Open pre-trained transformer language models. *arXiv preprint arXiv:2205.01068* (2022).